

PAPER • OPEN ACCESS

Lanczos steps to improve variational wave functions

To cite this article: Federico Becca *et al* 2015 *J. Phys.: Conf. Ser.* **640** 012039

View the [article online](#) for updates and enhancements.

Related content

- [Time reversal and Lanczos iterations](#)
A A Oberai, G R Feijoo and P E Barbone
- [High-Doping Regime in a Planar Model for Strongly Correlated Electrons](#)
J. Bona, P. Prelovšek and I. Sega
- [Harnessing molecular excited states with Lanczos chains](#)
Stefano Baroni, Ralph Gebauer, O Bari Malciolu *et al.*

Recent citations

- [Quantum State Complexity in Computationally Tractable Quantum Circuits](#)
Jason Iaconis
- [Spin Liquid versus Spin Orbit Coupling on the Triangular Lattice](#)
Jason Iaconis *et al*
- [Spin liquid nature in the Heisenberg, J₁J₂triangular antiferromagnet](#)
Yasir Iqbal *et al*



ECS **240th ECS Meeting**
Oct 10-14, 2021, Orlando, Florida

Register early and save up to 20% on registration costs

Early registration deadline Sep 13

REGISTER NOW

Lanczos steps to improve variational wave functions

Federico Becca¹, Wen-Jun Hu², Yasir Iqbal³, Alberto Parola⁴, Didier Poilblanc⁵, and Sandro Sorella¹

¹ Democritos National Simulation Center, Istituto Officina dei Materiali del CNR and SISSA-International School for Advanced Studies, Via Bonomea 265, I-34136 Trieste, Italy

² Department of Physics and Astronomy, California State University, Northridge, California 91330, USA

³ Institute for Theoretical Physics and Astrophysics, Julius-Maximilian's University of Würzburg, Am Hubland, D-97074, Würzburg, Germany

⁴ Dipartimento di Scienza e Alta Tecnologia, Università dell'Insubria, Via Valleggio 11, I-22100 Como, Italy

⁵ Laboratoire de Physique Théorique UMR-5152, CNRS and Université de Toulouse, F-31062 Toulouse, France

E-mail: becca@sissa.it

Abstract. Gutzwiller-projected fermionic states can be efficiently implemented within quantum Monte Carlo calculations to define extremely accurate variational wave functions for Heisenberg models on frustrated two-dimensional lattices, not only for the ground state but also for low-energy excitations. The application of few Lanczos steps on top of these states further improves their accuracy, allowing calculations on large clusters. In addition, by computing both the energy and its variance, it is possible to obtain reliable estimations of exact results. Here, we report the cases of the frustrated Heisenberg models on square and Kagome lattices.

1. Introduction

Obtaining accurate results in strongly-correlated systems remains an extremely difficult task in systems where the sign-problem prevents one to use numerically exact quantum Monte Carlo methods. [1] In the recent past, a large variety of numerical approaches have been proposed and devised to study simple models of interacting electrons on the lattice. Among the most promising ones, we mention post density-matrix renormalization group (DMRG) techniques, based upon tensor networks. [2, 3] As far as insulating phases are concerned, one important issue is to describe Mott insulators, in which the insulating character is driven by the strong electron-electron interaction. When lowering the temperature, the general expectation is that some symmetry-breaking phenomena take place, leading for example to magnetic or Peierls (i.e., dimerized) phases. In two spatial dimensions, a continuous symmetry cannot be spontaneously broken at finite temperatures; still, the ground state may possess magnetic long-range order. In this regard, the existence of quantum spin liquids, i.e., states that do not break any symmetry down to zero temperature, in two dimensions represents a fascinating problem. The key feature to impede long-range ordering is given by the presence of frustrating interaction, namely the presence of competing super-exchange couplings that strongly enhance quantum fluctuations. The simplest example that captures the low-energy physics of Mott insulators and may give rise



to spin-liquid ground states is the frustrated Heisenberg model:

$$\mathcal{H} = J_1 \sum_{\langle ij \rangle} \mathbf{S}_i \cdot \mathbf{S}_j + J_2 \sum_{\langle\langle ij \rangle\rangle} \mathbf{S}_i \cdot \mathbf{S}_j, \quad (1)$$

where both J_1 and J_2 are positive and \mathbf{S}_i are spin-1/2 operators at each lattice site i ; $\langle ij \rangle$ and $\langle\langle ij \rangle\rangle$ denote sum over nearest-neighbor and next-nearest-neighbor sites, respectively. Here, we consider both the square and Kagome lattices with N sites: $N = L \times L$ for the square lattice and $N = 3 \times L \times L$ for the Kagome lattice. All energies are given in units of J_1 .

The ground state properties of these two models have been widely debated in the past twenty years, with contradictory results. Recent DMRG calculations suggest that the ground state on the Kagome lattice for $J_2 = 0$ is a gapped Z_2 spin liquid, [4] while the ground state of the $J_1 - J_2$ model on the square lattice is a gapless spin liquid for $0.45 < J_2/J_1 < 0.5$ and a (gapped) valence-bond solid for $0.5 < J_2/J_1 < 0.6$. [5] Here, we present a variational Monte Carlo method to assess ground-state properties of these models. The starting variational wave functions can be substantially improved by the application of few Lanczos steps, which can be easily affordable for rather large clusters (i.e., few hundreds sites). Moreover, the calculation of both the energy and its variance makes it possible to perform a zero-variance extrapolation to estimate exact energies, not only for the ground state but also for low-energy excitations. [6, 7, 8]

2. Variational wave functions

The variational wave functions are defined through the mean-field Hamiltonian for the Abrikosov-fermion representation of the spin-1/2 operators: [9]

$$\mathcal{H}_{MF} = \sum_{i,j,\sigma} (t_{i,j} + \mu \delta_{ij}) c_{i,\sigma}^\dagger c_{j,\sigma} + \sum_{i,j} (\eta_{i,j} + \zeta \delta_{ij}) (c_{i,\uparrow}^\dagger c_{j,\downarrow}^\dagger + c_{j,\uparrow}^\dagger c_{i,\downarrow}^\dagger) + h.c., \quad (2)$$

where for each bond (i, j) there are hopping $t_{i,j}$ and/or pairing $\eta_{i,j}$ terms; on-site terms, i.e., a real chemical potential μ and/or a complex pairing ζ , may be also considered. Given any eigenstate $|\Psi_{MF}\rangle$ of the mean-field Hamiltonian (2), a physical state for the spin model can be obtained by a projection onto the subspace with one fermion per site:

$$|\Psi_v\rangle = \mathcal{P}_G |\Psi_{MF}\rangle, \quad (3)$$

where $\mathcal{P}_G = \prod_i (n_{i,\uparrow} - n_{i,\downarrow})^2$ is the Gutzwiller projector, $n_{i,\sigma} = c_{i,\sigma}^\dagger c_{i,\sigma}$ being the local density. The flexibility of this approach is given by the fact that *different* spin liquids, having for example $U(1)$ or Z_2 gauge structure and gapped or gapless spinon spectrum, may be obtained by changing the pattern of the $t_{i,j}$'s and the $\eta_{i,j}$'s. [10] Moreover, dimerized or chiral states can be also easily obtained within this approach. [11, 12]

In the following, we will consider the square lattice with $J_2/J_1 = 0.5$ and the Kagome lattice with both $J_2 = 0$ and $J_2 = 0.25$, corresponding to cases where the high frustration may stabilize fully symmetric spin liquids. For the square lattice, we will consider a state that is obtained by taking a real pairing η_{xy} (with d_{xy} symmetry) on top of the $U(1)$ state with nearest-neighbor hopping t and real pairing $\eta_{x^2-y^2}$ (with $d_{x^2-y^2}$ symmetry). The d_{xy} term is responsible for breaking the $U(1)$ gauge symmetry down to Z_2 . Restricting this coupling along the $(\pm 2, \pm 2)$ bonds implies four Dirac points in the mean-field spectrum. [6] For the Kagome lattice, we will consider the $U(1)$ state that is described by nearest-neighbor real hoppings such to have 0 magnetic flux through triangles and π flux through hexagons. [13] At the mean-field level, there are gapless excitations at two Dirac points. A slight improvement of the energy can be achieved by considering a next-nearest-neighbor real hopping. [11] A gapped wave function, corresponding

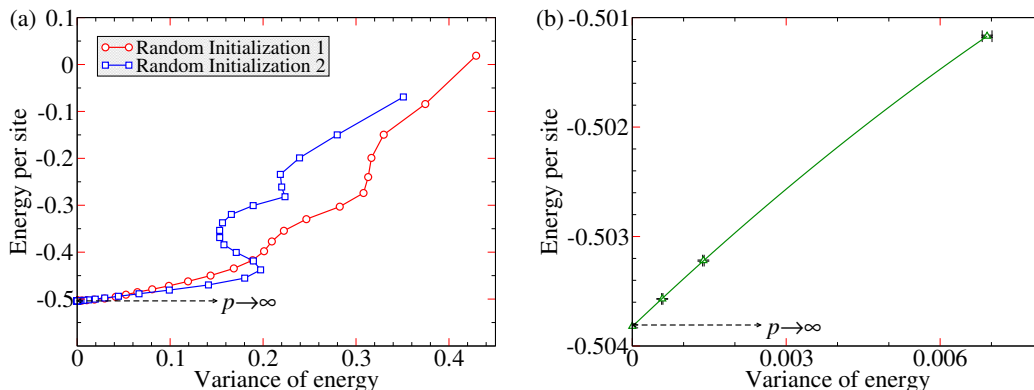


Figure 1. The energy per site versus the energy variance per site for the J_1 – J_2 Heisenberg model on the square lattice with $J_2/J_1 = 0.5$ and $L = 6$. Exact Lanczos diagonalizations starting from two random initializations (a) and quantum Monte Carlo calculations starting from the best variational state (3) (b) are reported. Points correspond to different values of p .

to a Z_2 spin liquid (labelled by $Z_2[0, \pi]\beta$) can be obtained by adding on-site and next-nearest-neighbor pairing terms. [14] A gapless spin liquid with a large Fermi surface (labeled by uniform RVB) is obtained when no magnetic fluxes are present.

Within this formalism, it is straightforward to construct not only an Ansatz for the ground state but also for low-energy excitations. In this respect, it is useful to consider a particle-hole transformation for the down electrons on the mean-field Hamiltonian (2), i.e., $c_{i,\downarrow}^\dagger \rightarrow c_{i,\downarrow}$, such that the transformed Hamiltonian conserves the total number of particles. Then, the ground state is obtained by filling the lowest N orbitals, with suitable boundary conditions (either periodic or anti-periodic) in order to have a unique mean-field state. Spin excitations can be obtained by creating the appropriate Bogoliubov quasi-particles (spinons) and possibly switching boundary condition. In particular, it is easy to construct a unique and real wave function containing four spinon excitations with total momentum $k = (0, 0)$, while generic $S = 1$ excitations would require complex wave functions. Therefore, we will consider the case of a $S = 2$ excitation with momentum $k = (0, 0)$, for both the square and the Kagome lattices. By computing separately the energies of the $S = 0$ and $S = 2$ states, the spin gap Δ_2 is studied as a function of the cluster size.

3. Lanczos step procedure

In order to systematically improve the variational wave functions, we can apply a number p of Lanczos steps to the starting variational wave function:

$$|\Psi_p\rangle = \left(1 + \sum_{m=1}^p \alpha_m \mathcal{H}^m\right) |\Psi_v\rangle, \quad (4)$$

where α_m are p additional variational parameters. Clearly, whenever $|\Psi_v\rangle$ is not orthogonal to the exact ground state, $|\Psi_p\rangle$ converges to it for large p . Unfortunately, on large sizes, only few steps can be efficiently afforded: here, we consider the case with $p = 1$ and $p = 2$ ($p = 0$ corresponds to the original variational wave function). Furthermore, an estimate of the exact energy may be obtained by the variance extrapolation. Indeed, for accurate variational states $|\Psi_p\rangle$ with energy E_p and variance σ_p^2 , it is easy to prove that

$$E_p \approx E_{\text{ex}} + \text{const} \times \sigma_p^2, \quad (5)$$

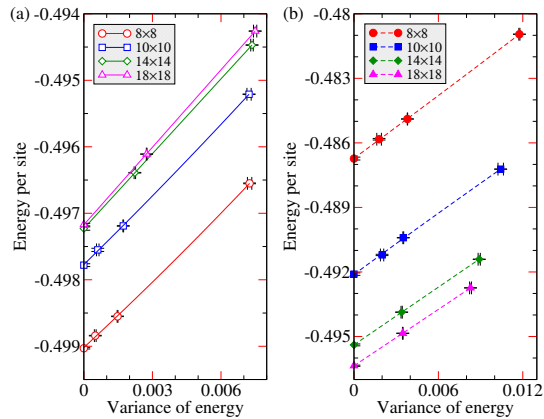


Figure 2. Energies per site for $S = 0$ (a) and $S = 2$ (b) versus the energy variance per site for the Heisenberg model on the square lattice with $J_2/J_1 = 0.5$. The initial state is the best variational Ansatz (3). The variance extrapolated results are also shown.

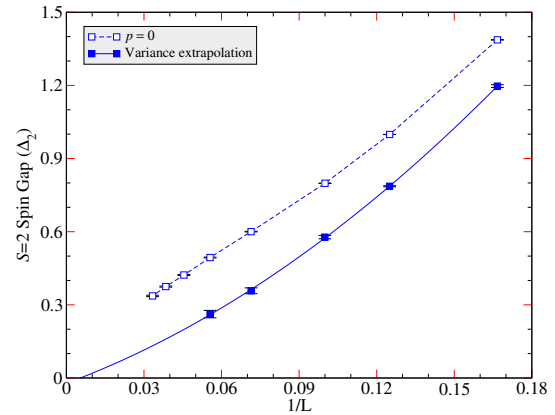


Figure 3. The size scaling of the $S = 2$ spin gap for the best variational wave function and the zero-variance extrapolation on the square lattice with $J_2/J_1 = 0.5$. The thermodynamic extrapolation gives $\Delta_2 = -0.04(5)$.

where

$$E_p = \frac{\langle \Psi_p | \mathcal{H} | \Psi_p \rangle}{N}, \quad (6)$$

$$\sigma_p^2 = \frac{\langle \Psi_p | \mathcal{H}^2 | \Psi_p \rangle - \langle \Psi_p | \mathcal{H} | \Psi_p \rangle^2}{N}, \quad (7)$$

are the energy and variance per site, respectively. Therefore, the exact energy E_{ex} may be extracted by fitting E_p versus σ_p^2 and performing a zero-variance extrapolation.

It should be emphasized that the Lanczos step procedure of Eq. (4) is not size consistent if p is not increased with the number of sites N . Indeed, both the energy and variance improvements with respect to the original state $|\Psi_v\rangle$ vanish for $N \rightarrow \infty$ and fixed p . Nevertheless, it is remarkable that a sizable improvement is obtained even for rather large clusters with few hundred sites. By contrast, the zero-variance extrapolation remains size consistent, as shown below.

4. Monte Carlo sampling

By using the variational Monte Carlo technique, the properties of the Gutzwiller-projected wave function can be easily assessed. Indeed, expectation values of any operator \mathcal{O} , including \mathcal{H} , are given by:

$$\frac{\langle \Psi_p | \mathcal{O} | \Psi_p \rangle}{\langle \Psi_p | \Psi_p \rangle} = \sum_x \frac{\langle \Psi_p | x \rangle \langle x | \mathcal{O} | \Psi_p \rangle}{\langle \Psi_p | \Psi_p \rangle} = \sum_x \frac{|\langle \Psi_p | x \rangle|^2 \langle x | \mathcal{O} | \Psi_p \rangle}{\langle \Psi_p | \Psi_p \rangle \langle x | \Psi_p \rangle}, \quad (8)$$

where $\{|x\rangle\}$ represents a complete and orthogonal basis. By interpreting $P(x) = \langle \Psi_p | x \rangle^2 / \langle \Psi_p | \Psi_p \rangle$ as a probability distribution, a Markov chain can be constructed to sample Eq. (8). In particular, the Gutzwiller projector is automatically implemented by taking $\{|x\rangle\}$ written in terms of electron configurations in real space with only singly-occupied sites. Within the fermionic representation, an efficient Metropolis algorithm can be implemented with local electron moves, e.g., spin flips, $|x\rangle \rightarrow |x'\rangle$. For $p = 0$, whenever few electrons are moved, the computational cost of $P(x')/P(x)$ only requires $O(1)$ operations, while the updating when a new configuration is accepted requires $O(N^2)$ operations. In order to have uncorrelated electron

configurations, N moves must be done, so that the variational algorithm scales like $O(N^3)$. When the first Lanczos step is implemented, the only extra cost is that $P(x')/P(x)$ scales as $O(N)$, while the second Lanczos step gives $O(N^2)$; in both cases the updating algorithm remains $O(N^2)$. Therefore, up to $p = 2$, the variational calculations have the same computational effort as the $p = 0$ case. In some cases, in order to have a stable simulation for p Lanczos steps, it is important to adopt a regularization scheme to avoid vanishingly small determinants. Here, we consider to sample configurations $|x\rangle$ such that

$$\sum_{x' \neq x} \left| \frac{\langle x | \mathcal{H} | x' \rangle \langle x' | \Psi_v \rangle}{\langle x | \Psi_v \rangle} \right| < \frac{N}{\epsilon}. \quad (9)$$

A finite ϵ represents a restriction of the Hilbert space and, therefore, slightly raises the variational energy. On the other hand, a finite ϵ makes the simulation more stable, since it eliminates large statistical fluctuations. Therefore, one must find a compromise between these two effects and fix a value that optimizes the results: empirically, we find that the best choice is given by ϵ ranging from 10^{-6} to 10^{-5} .

5. Results

We start by showing how the Lanczos step procedure and the variance extrapolation work for a case where exact diagonalizations are also available, namely the Heisenberg model on the square lattice with $L = 6$ and $J_2/J_1 = 0.5$. In Fig. 1, we report the calculations for the ground state in two different cases, either by starting from random initial states (i.e., what is usually done in the Lanczos method) or by initializing with the best variational wave function (3). While in the former cases, many Lanczos steps are needed to reach a good energy per site and, therefore, also the linear regime of Eq. (5), the latter one gives excellent results even with two steps, the zero-variance extrapolation being exact within the statistical error. We would like to stress that abrupt reductions of the energy, with almost constant variance, or even non-monotonic behaviors, can appear when the initial wave function has large overlaps with excited states.

By using the best Gutzwiller projected state, we can extend the Lanczos step procedure to larger systems, where exact diagonalizations are not possible. In Fig. 2, we report the calculations for both the $S = 0$ ground state and the $S = 2$ excitation. Calculations are performed up to $L = 10$ with $p = 0, 1$, and 2 , and up to $L = 18$ with $p = 0$ and 1 . Even though it is visible that the energy/variance gain reduces when increasing L , the slope of the fit remains similar, allowing a size-consistent zero-variance extrapolation. From these results, the $S = 2$ gap is shown in Fig. 3. We expect a vanishing gap in the thermodynamic limit for the variational calculations with $p = 0$, since the Z_2 gauge structure is not expected to alter the mean-field properties. [10] However, our numerical results up to $L = 30$ cannot definitively confirm this fact. Most importantly, the zero-variance extrapolation for the gap suggests that the frustrated Heisenberg model on the square lattice is gapless for $J_2/J_1 = 0.5$.

Let us move to the Kagome lattice. In Fig. 4, we report the variance extrapolation for a small lattice with 48 sites (i.e., $L = 4$) for both $J_2 = 0$ and $J_2/J_1 = 0.25$. For the former case, no matter what is the initial state (gapless with Dirac points or a large Fermi surface, or even gapped), the extrapolated energy is the same, within the statistical errors. Notice, however, that the actual values of the initial energies and variances are quite different for these three cases. By contrast, for the case with $J_2 = 0.25$, a rather different behavior is found when starting from the $U(1)$ Dirac state or the Z_2 gapped one. Remarkably, although the latter one gives a slightly better variational energy for $p = 0$, the Lanczos extrapolation performs much better for the Dirac state, where a smooth fit is possible. Instead, for the $Z_2[0, \pi]\beta$ state, the second Lanczos step makes a sensible energy gain, while the variance does not improve. This behavior is reminiscent of what is seen when the initial wave function has some large overlap with excited

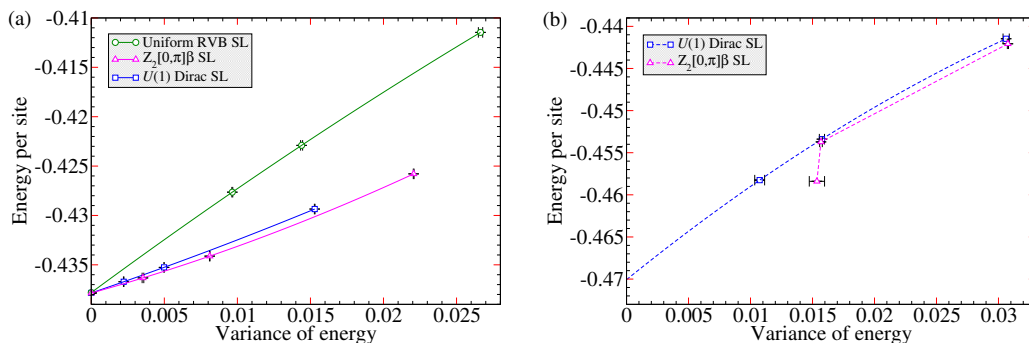


Figure 4. Energies per site for the $S = 0$ states for the Heisenberg model on the Kagome lattice on 48 sites (i.e., $L = 4$) for $J_2 = 0$ (a) and $J_2/J_1 = 0.25$ (b). Both the $U(1)$ Dirac spin liquid and the gapped $Z_2[0, \pi]\beta$ (for which the next-nearest-neighbor pairing η is fixed to 1) spin liquid are reported; for $J_2 = 0$, the uniform RVB state with vanishing magnetic fluxes is also reported.

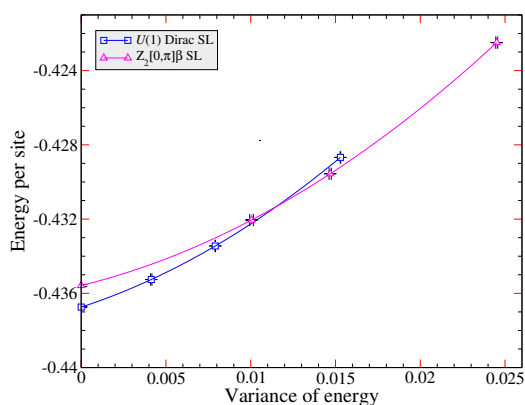


Figure 5. The energy per site versus the variance per site on the Kagome lattice with $L = 8$ and $J_2 = 0$ for the $U(1)$ Dirac spin liquid and the gapped $Z_2[0, \pi]\beta$ spin liquid.

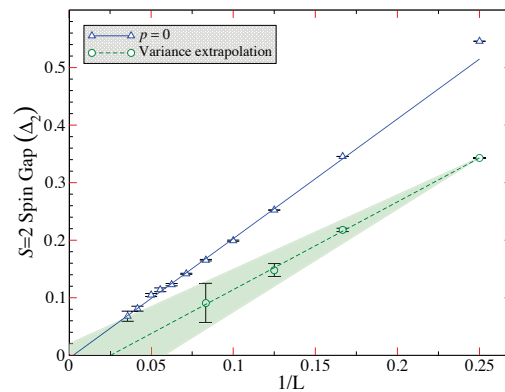


Figure 6. The size scaling of the $S = 2$ spin gap for the $U(1)$ Dirac state and the zero-variance extrapolation on the Kagome lattice with $J_2 = 0$. The thermodynamic extrapolation gives $\Delta_2 = -0.04(6)$.

states (see Fig. 1 for the square lattice). The evidence that the $Z_2[0, \pi]\beta$ state is not a good approximation even when $J_2 = 0$ is reported in Fig. 5. For $L = 8$, the Lanczos extrapolation of the $U(1)$ Dirac spin liquid gives a better energy than the one obtained from the Z_2 state.

By performing a size-scaling extrapolation of the gap by using the $U(1)$ Dirac state, we obtain the results shown in Fig. 6. First of all, it is clear that the Gutzwiller projector does not open a spin gap on top of the Dirac state: this is a non-trivial outcome, given the fact that a $U(1)$ gauge structure may give rise to strong interactions among spinons that may completely change the mean-field picture. Most importantly, also after the Lanczos step extrapolation, the system is compatible with a gapless spectrum.

6. Conclusions

In summary, we have shown that extremely accurate calculations for the energy per site are possible in frustrated two-dimensional lattice by using variational wave functions that are built from Abrikosov fermions. Few Lanczos steps can be applied to the pure variational state, giving a remarkable energy gain, also for clusters with few hundreds sites. Moreover, performing a

zero-variance extrapolation, it is possible to obtain accurate values of the exact energies, not only for the ground state but also for excited states.

References

- [1] Kaul R K, Melko R G and Sandvik A W 2013 *Annu. Rev. Con. Mat. Phys.* **4** 179
- [2] Schollwoek U 2011 *Annals of Physics* **326** 96
- [3] Orus R 2014 *Annals of Physics* **349** 117
- [4] Yan S, Huse D A and White S R 2011 *Science* **332** 1173
- [5] Gong S S, Zhu W, Sheng D N, Motrunich O I and Fisher M P A *Phys. Rev. Lett.* **113** 027201
- [6] Hu W J, Becca F, Parola A and Sorella S 2013 *Phys. Rev. B* **88** 060402
- [7] Iqbal Y, Becca F, Sorella S and Poilblanc D 2013 *Phys. Rev. B* **87** 060405
- [8] Iqbal Y, Poilblanc D and Becca F 2014 *Phys. Rev. B* **89** 020407
- [9] Baskaran G and Anderson P W 1988 *Phys. Rev. B* **37** 580
- [10] Wen X G 2002 *Phys. Rev. B* **65** 165113
- [11] Iqbal Y, Becca F and Poilblanc D 2011 *Phys. Rev. B* **83** 100404
- [12] Bieri S, Messio L, Bernu B and Lhuillier C 2014 *Preprint* arXiv:1411.1622
- [13] Ran Y, Hermele M, Lee P A and Wen X G 2007 *Phys. Rev. Lett.* **98** 117205
- [14] Lu Y M, Ran Y and Lee P A 2011 *Phys. Rev. B* **83** 224413